FIRE PERFORMANCE OF EXTERNAL SEMI-RIGID COMPOSITE JOINTS

PETER SCHAUMANN[1], BIN ZHAO[2], OLIVER BAHR[3] and CHRISTOPHE RENAUD[4]

ABSTRACT

This contribution deals with the fire performance of external semi-rigid composite joints. First, the design principles of two newly developed joints are explained. Four fire tests were carried out to investigate the fire performance of the new joints. To study local phenomena in the joint, a three-dimensional numerical model was established with the Finite Element code Abaqus for one joint type. The data obtained from the fire tests were used to validate the model. It is shown that the model is suitable to predict the fire performance of the chosen external semi-rigid composite joint. Thus, parametric studies were conducted to extend the parameter set of the fire tests. Based on the results of the numerical studies, the paper concludes with recommendations for the design of the developed composite joints.

1. INTRODUCTION

Current Eurocodes for the fire design are limited to braced structures. However, a large market is seen for unbraced composite frames with three storeys at most and fire resistance classes up to R60. The frames could be used for instance in office, industrial, and school buildings. Thus, the ongoing European project 'Unbraced Composite Structures in Fire' addresses this topic [1]. The numerical investigations performed within the scope of this project showed that the joint behaviour is crucial for the overall fire performance of the frames. Examplary numerical simulations of a fire-exposed unbraced composite frame at failure stage can be found [2].

However, even in composite constructions the connections between perimeter columns and beams are mostly pure steel connections. Therefore the authors investigated the fire performance of external composite joints experimentally and numerically. Two different types of composite joints were considered. As presented in Figure 1, the first type of composite joint is a full composite solution without any additional fire protection. The second type of joint is more conventional with reinforced concrete-filled steel tubes and normal composite beams. Four fire tests on composite joints were carried out by CTICM. The joints were designed to achieve a fire rating of 60 min. The Institute for Steel Construction established advanced calculation models of the joints in the non-linear software Safir and Abaqus. For the former, please refer to [2]. The latter is presented in this contribution and in [3].

[1] Professor, Leibniz University Hannover, Institute for Steel Construction, Hannover, Germany, email: schaumann@stahl.uni-hannover.de.
[2] Dr., Head of the Fire Research Section, CTICM, 91193 Saint-Aubin, France, email: binzhao@cticm.com.
[3] Research Assistant, Leibniz University Hannover, Institute for Steel Construction, Hannover, Germany, email: bahr@stahl.uni-hannover.de *(corresponding author)*.
[4] Dr., CTICM, 91193 Saint-Aubin, France, email: chrenaud@cticm.com.

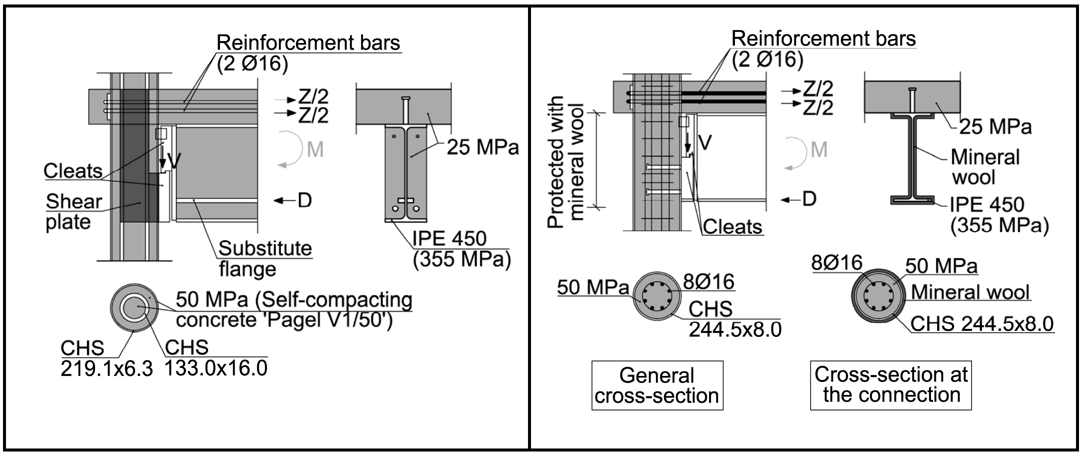

(a) **(b)**

Figure 1 - Design drawing of composite joint with concrete-filled double skin steel tubular (CFDST) columns **(a)** and of protected composite joint with concrete-filled steel tubular (CFST) columns **(b)**.

2. DESIGN PRINICIPLES OF THE DEVELOPED JOINTS

As presented in Figure 1(a), the first type of composite joint is a full composite solution without any additional fire protection. This solution consists of concrete-filled double skin steel tubular (CFDST) columns combined with partially concrete encased composite beams. A shear plate that is welded to the inner tube transfers the load from the beam into the inner tube. Under fire condition, the inner tube progressively bears the loads due to the quick heating of the outer tube. In this context, it is referred to the extensive research on CFDST columns conducted by Zhao and Han [4].

The second type of joint is more conventional with reinforced concrete-filled steel tubular (CFST) columns and normal fire-protected composite beams. In consequence, the fire protection applied to the beams is extended to the joint zone, as it is shown in Figure 1(b). With cleats and additional studs penetrating the concrete core, this allows for transferring the high local forces into the column that result from the bending moment of the beam. Further details of the design of the joints are given in [3].

3. FIRE TESTS

3.1 Aim of the tests

Four isolated full-scale joint tests were carried out to study the fire performance of the new composite joints and to validate the established numerical models. For each joint type, two tests were conducted in the fire laboratory of Efectis France under the coordination of its parent company CTICM [5].

The tests were designed to study both global and local failure of the joints. The former clarified the performance of the joints in unbraced composite frames, whereas the last focused on their load-bearing and rotational capacity. Finally, the tests should ensure the theoretical design of the joints for a fire rating of at least 60 min to ISO standard fire.

3.2 Test specimens

The dimensions of the test specimens were chosen such that the test specimens could be integrated in the furnace. Furthermore, realistic cross-sections were taken from the design of a one-bay three-storey unbraced composite frame with span of 12 m (see [2], Figure 1). Table I gives the key test parameters.

Steel tensile coupon tests and concrete compression tests were carried out to determine the actual mechanical material properties at ambient temperature. For the steel specimens, Table I shows the average proof limit $R_{p0.2}$, which is the stress at 0.2% residual strain.

The CFDST columns of the composite joints (specimens 'C1' and 'C2' in Table I) were concreted with self-compacting concrete type 'V1/50' from the German company 'Pagel Spezial-Beton' of strength class C50/55. For the CFST columns (specimens 'P1' and 'P2'), normal-weight of strength class C50/55was used. The beam was protected by one layer of mineral wool 'Insulfrax S' with a thickness of 25 mm. The protection was extended around the column and covered the connection over the full height of the beam. As shown in Figure 1, an IPE450 beam with a concrete slab of 160 mm height was used in all four tests. The slab and concrete between the flanges had nominal strength class of C25/30.

3.3 Test set-up

The base of the columns was fully restrained. Accompanying numerical studies in [2] showed that a fixed base support is crucial for the fire performance of the unbraced frames. In the fire tests, the pinned joint at the top of the column enforces the contraflexure that occurs at each storey level of realistic multi-storey frames. In longitudinal direction, the columns were free to move. To prevent out-of-plane bending of the joints, two additional profiles braced the column head. Some space was given to ensure that there was no initial contact between the column and the bracing.

3.4 Instrumentation and loading

As indicated in Figure 2(a), wire sensors were placed at the beginning and near the end of the beams. Additional sensors on the columns measured the axial deformation. Furthermore, the inclinations were measured by angular sensors. About eighty thermocouples were installed on each test specimen in different sections of the joint, beam, and column to record temperatures. Furthermore, sixteen plate thermometers captured temperatures inside the furnace. A special high temperature video camera was put inside the furnace to record visually the specimen deformations versus time.

Table I. Material properties.

Test	Steel strength $R_{p0.2}$ (MPa)			Reinforcement (MPa)	Concrete strength (MPa)	
	Outer tube	Inner tube	Beam Flange/Web	Slab	Column	Beam and slab
C1	369	422	374/397	659	74.0	33.5
C2	371	375				
P1	368	./.	374/397	659	86.5	33.5
P2	379	./.				

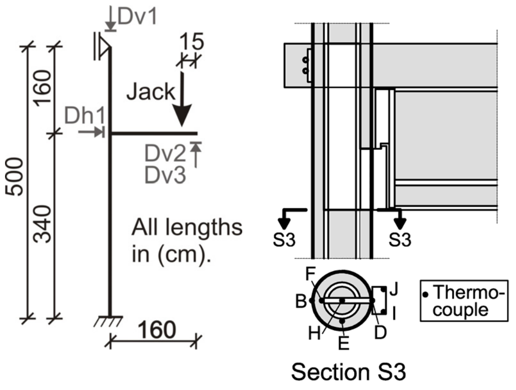

(a) (b)

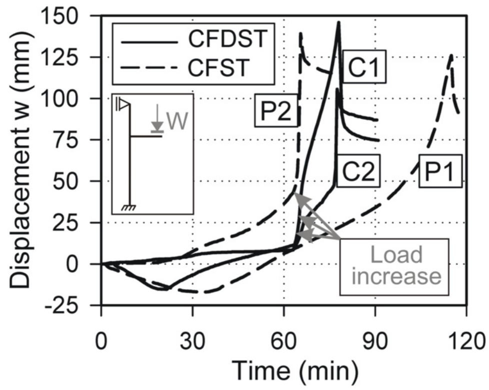

Figure 2 - Static system of the fire tests **(a)**; section for the temperature measurements **(b)**.

Figure 3 - Displacement at the beam end for the different joint tests.

A loading device was developed allowing the jack to follow the sway of the test specimens. Therefore the jack was fixed to a movable beam on a crane trolley. All specimens were exposed to ISO standard fire for at least 60 min.

Before fire exposure, the load was applied manually with help of a hydraulic jack at the end of the beam as shown in Figure 2(a). The load was continuously monitored and manually regulated during the fire test. During the first 60 minutes of the test, the applied moment at the joint M_φ remained in three of four tests well below the nominal moment. This was to ensure that sufficient thermal data could be gained for the validation of the established numerical model. After 60 min, the load was increased within three tests as reported in Table II. The tests had to be stopped when either the deformations became too large or when the inclination of the jack was exceeded. Table II also shows the nominal load ratio for the different joint tests, which is defined as the ratio of the resulting moment into the joint during the fire test to the nominal moment resistance of the joint at room temperature.

To induce the global failure mode described in section 3.1, the total length of the circular CFST and CFDST columns in the furnace was exposed to ISO standard fire (see Figure 4). In contrast to this, for the local failure mode only the upper 750 mm of the column in the furnace were exposed to heating (see Figure 5). The rest of the column was protected with a layer of 25 mm mineral wool. After failure, the load was removed. All tests were continued to the next fire rating time to collect thermal data for the numerical validation.

3.5 Results

Figure 3 shows the evolution of the deflection 'w' at the end of the slab . In the first twenty minutes, thermal expansion of the columns can be observed. The expansion is less concise for the specimens where local failure was induced because their heated length was only 750 mm. In general, all joints failed with the expected global or local failure mode according to Figures 4 and 5.

Table II. Summary of test parameters.

Test	Outer tube	Inner tube	Applied load (kN)	Load ratio in the joint section (%)	Failure time (min)
C1	CHS 219.1×6.3	CHS 133.0 × 16.0	100 (140)*	83 (117)	78
C2	RHS 260×180×6.3	RHS 160×90×10.0	130 (200)**	109 (168)	78
P1	CHS 244.5×8.0	No inner tube.	75	63	115
P2	RHS 260×180×6.3	No inner tube.	100 (125)***	83 (105)	66

CHS denotes Circular Hollow Section and RHS denotes Rectangular Hollow Section.
Load was increased between *63-78 min, **63-68 min, and ***63-66 min, respectively.

In addition, the joints showed sufficient ductility between φ=80 mrad (test C2) and φ=100 mrad (test C1). Thus, the joints are appropriate to allow for the large rotations that occur into the joints of fire-exposed unbraced composite frames.

Furthermore, the tests confirmed that both joint types with CFDST and CFST columns are suitable for fire ratings of at least 60 min, which is even true for the tests with load ratios higher than the nominal load-bearing capacity. For the last, their high load-bearing capacity can be attributed to the overstrength of the reinforcement bars bent around the column (see Table I).

4. THREE-DIMENSIONAL FINITE ELEMENT MODEL

4.1 General description of the model, Finite Element type, and mesh

A three-dimensional Finite Element model of the circular external composite joint was established in Abaqus/Explicit to conduct parametric studies. Most of the mesh consists of six-node linear triangular prism elements C3D6 with an element size of about 30 mm. The more complex geometry near the column was meshed with four-node linear tetrahedron elements C3D4 with an element size around 20 mm.

4.2 Boundary conditions, load application, and interactions

Rigid bodies represent the lower and upper support, where end plates with thickness of 40 mm and 20 mm were used in the test, respectively. Same as in the fire tests, the lower support is constrained against all degrees of freedom, whereas the upper support allows for rotation and axial movement of the column. The load was applied at a distance of 150 mm from the end of the cantilever, corresponding to the load configuration in the fire test. In the test, a circular knuckle was installed between the head of the jack and the slab. In the model, a rectangular pressure of same area was applied to simplify the mesh. The applied load in the model strictly followed the recorded load history of the test. Full contact was assumed between all steel and concrete elements.

4.3 Material modeling

For the steel and reinforcement bars, constitutive laws from Eurocode 4-1-2 [6] were used. The concrete damaged plastic model was adopted to simulate the concrete [7-9]. It describes the inelastic behaviour of concrete with concepts of isotropic damage combined with isotropic tensile and compressive plasticity. Real stress-strain relationships were used for all materials.

4.4 Validation of the model

Cross-sectional temperatures were recorded from thermocouples placed at six different sections during the fire tests. In general, the established numerical model accurately predicts the temperatures obtained in the fire tests. In this contribution, section S3 in Figure 2(b) was chosen. Figure 6(a) shows that the numerical model predicts reasonably the evolution of cross-sectional temperatures.

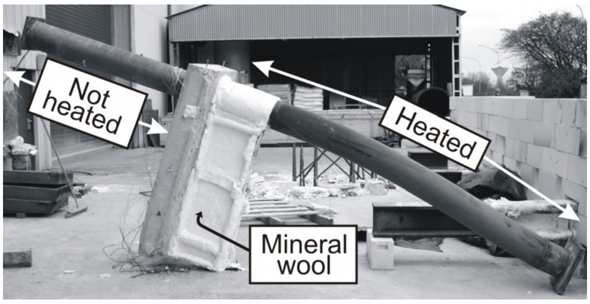

Figure 4 - Specimen P1 after the fire test (global failure mode).

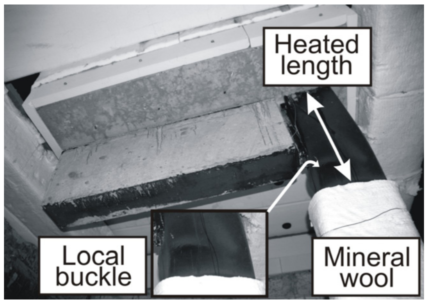

Figure 5 - Specimen C2 after the fire test (local failure mode).

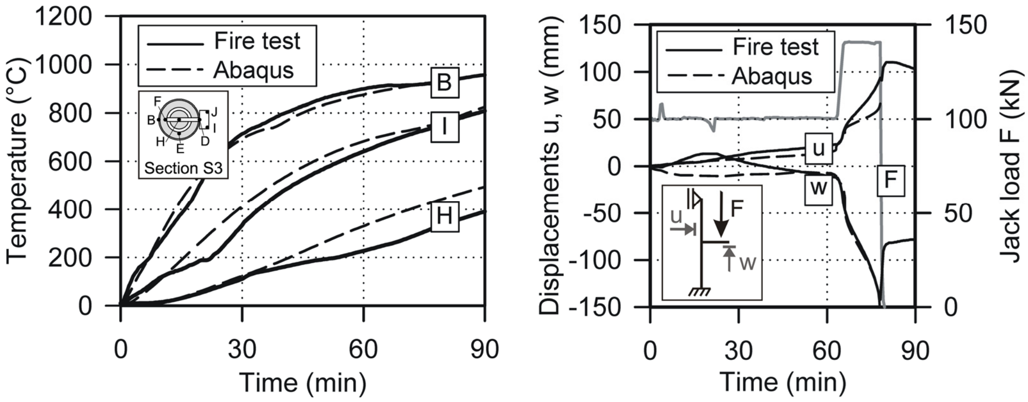

(a) **(b)**

Figure 6 - Comparison between cross-sectional temperatures **(a)** and displacements **(b)** in the fire test of the circular joint 'C1' with CFDST column and the Abaqus results.

Figure 6(b) shows the deflection of the slab at the end of the cantilever beam as well as the horizontal movement of the column, where the displacement transducers are positioned according to Figure 2(a). Furthermore, the jack load 'F' is depicted in Figure 6(b) with its magnitude on the secondary vertical axis. As it can be seen, the applied load was regulated to a value of 100 kN until 63 min. Afterwards, the load was linearly increased within three minutes to 140 kN and kept constant. The numerical calculation resulted in 77 min failure time compared to 78 min in the fire test. In general, there was a sharp increase of deformations when the applied load was increased to 140 kN. As shown in Figure 6(b), the numerical results for the horizontal movement 'u' of the column and the displacement ‘w’ at the end of the slab are close to the results obtained from the fire test. For a detailed discussion of the validation, it is referred to [3].

5. INFLUENCE OF THE LOCATION OF THE FIRE

Numerical studies were conducted to investigate the effect of the location of the fire on the fire performance of the circular external composite joint. The fire performance of the joint was evaluated in terms of the global deformations and local stresses in the shear panel. The latter was chosen since it plays a crucial for the fire performance of the joint [3]. Figure 7(a) depicts the temperature field of the inner tube, shear panel, and cleat after 60 min exposure to ISO standard fire in the ground and first storey. The investigation showed that the cross-sectional temperatures in the penetrating shear panel are governed by the fire in the ground storey, whereas the influence of thermal action in the upper storey is negligible.

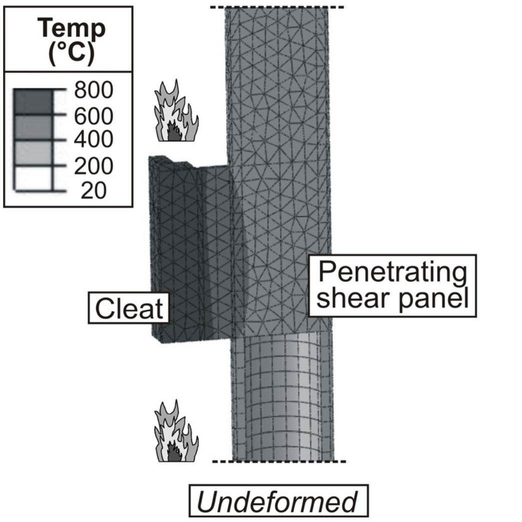

(a) Temperature distribution in the shear panel for fire in both storeys (concrete not shown).

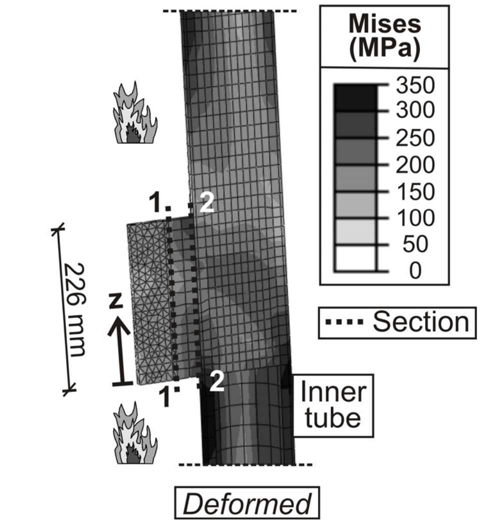

(b) Von Mises stresses in the shear panel for fire in both storeys (concrete not shown).

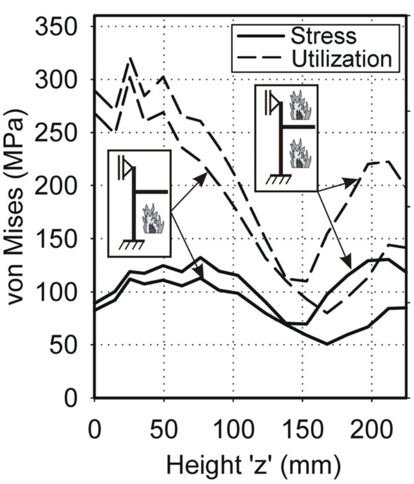

(c) Stress and utilization in section 1-1 of the shear panel depending on position 'z'.

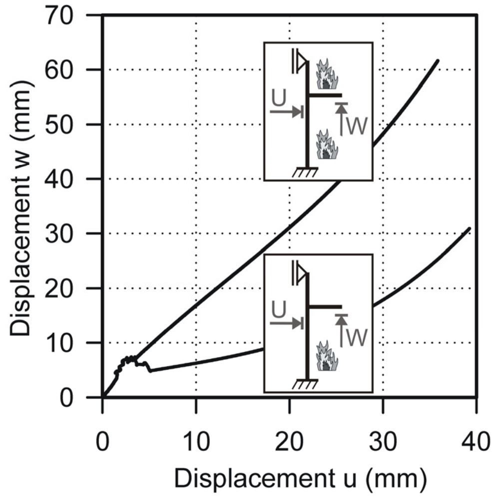

(d) Displacement w of the beam plotted versus sway u of the column.

Figure 7 - Numerical results for the influence of the location of the fire.

In addition, Figure 7(b) shows the two deformed sections '1-1' and '2-2', where von Mises stresses were evaluated after 60 min fire exposure. The study showed that because of its higher cross-sectional temperatures section '1-1' at the cleat was more critical than section '2-2' at the thermally protected inner tube. The heating reduces the effective yield stress $f_{y,\theta}$. For this reason, Figure 7(c) shows the von Mises yield stress σ_v for multiaxial loading conditions for the critical section '1-1' and for both regarded fire scenarios. The stresses are plotted over the height 'z' of the shear panel, which is depicted in Figure 7(b). Furthermore, the utilization is given in Figure 7(c), which was defined as the ratio of the von Mises stress and the effective uniaxial yield stress $f_{y,\theta}$ of the fire-exposed steel with nominal strength of 355 MPa. Results for section 2-2 are not shown because the maximum utilization was 74% and hence not critical.

From the utilization, it may be concluded that the shear panel that is exposed to fire only from the ground storey offers more residual load-bearing capacity in its upper part. Contraty, for fire in both storeys the panel was close to yielding and hence local failure of the joint. This conclusion is underlined by Figure 7(d) that plots the deflection 'w' of the beam versus the sway 'u' of the column. Accordingly, the deflection ‘w’ for fire in both storeys was significantly higher than for fire in the ground storey only. Besides the higher utilization of the shear panel, one main reason is that the continuous column provides less moment resistance if it is exposed to fire in both storeys.

6. SUMMARY AND OUTLOOK

Based on the information presented, the following conclusions may be drawn:

- It has been shown that the established numerical modeling predicts the fire performance of the investigated composite joints with a good accuracy. Altogether, the investigations showed that the developed semi-rigid joints may provide a promising alternative to common joints for perimeter columns.
- The two developed external semi-rigid composite joints are suitable for fire ratings of at least 60 min exposure to ISO standard fire, which was confirmed by four full-scale fire tests.
- Fire in both storeys is more critical than in one storey since it induces failure by yielding of the penetrating shear panel.

ACKNOWLEDGEMENTS

The work presented here has been carried out with a financial grant from the Research Fund for Coal and Steel (RFCS) of the European Community. The authors gratefully acknowledge the financial support and appreciate the intensive cooperation among the project partners. Furthermore, the authors would like to thank the company 'Pagel Spezial-Beton' for the supply of material and concreting of the test specimens in France and Germany.

REFERENCES

[1] European Commission. 2007-2010. Research project 'Unbraced Composite Structures in Fire' (UCoSiF). Research Fund for Coal and Steel, Contract N°RFSR-CT-2007-00044, Brussels.
[2] Schaumann, P. and Bahr, O., “A numerical model for unbraced composite frames in fire”, Structures in Fire 2010, Michigan, USA, 2010 *(accepted for publication)*.
[3] Schaumann, P. and Bahr, O., “Fire design of external semi-rigid composite joints”, ISTS13, Hong Kong, 2010 *(accepted for publication)*.
[4] Zhao, X.-L. and Han, L.-H., “Double skin composite construction”, Progress in Structural Engineering and Materials, Volume , pp. 93-102, 2004.
[5] Efectis France, “Fire test on composite external semi-rigid composite joints”, Test reports 09-U-538, 09-U-543, 09-U-554, and 09-U-559, 2009.
[6] European Committee for Standardization, EN 1994-1-2, “Design of composite steel and concrete structures, Part 1-2: General rules - Structural fire design”, 2006.
[7] Hillerborg, A., Modeer, M. and Petersson, P. E., “Analysis of crack formation and crack growth in concrete by means of fracture mechanics and Finite Elements”, Cement and Concrete Research, Volume 6, Issue 6, pp. 773-782, 1976.
[8] Lee, J. and Fenves, G. L., “Plastic-damage model for cyclic loading of concrete structures”, Journal of Engineering Mechanics, Volume 124, Issue 8, pp. 892-900, 1998.
[9] Lubliner, J., Oliver, S., Oller, S. and Oñate, E., “A plastic-damage model for concrete”, International Journal of Solids and Structures, Volume 25, Issue 3, pp. 229-326, 1989.